

# Reports

## Sodium Humate Solution Studied with Small-Angle X-Ray Scattering

**Abstract.** *Small-angle x-ray scattering analyses of sodium humate solutions indicate either that particles of two or more different sizes exist in solution or that all of the particles are the same size but consist of a dense core and a less dense outer shell. Fractionation on a molecular sieve chromatographic column suggests that the first possibility is the more likely of the two. The radius of gyration and molecular weight of the larger particles are respectively 110 Å and  $1 \times 10^6$  and those of the smaller particles 38 Å and  $2.1 \times 10^5$ . These particles are ellipsoidal.*

Humic acid is defined as the alkali-soluble, acid-insoluble organic fraction of soils. Various approaches to elucidate its structure (1, 2) involve, in addition to traditional methods, the more recent techniques of electron microscopy (3), electron paramagnetic resonance (4), and pyrolysis-gas chromatography (5). However, humate solutions have not been studied by small-angle x-ray scattering until now.

Small-angle x-ray scattering has proved useful in the study of solutions of colloidal-sized particles. We present here a report on the determination of the molecular weight, molecular volume, radius of gyration, possible shape factors, and dispersity of sodium humate in solution by small-angle x-ray scattering.

These factors may be calculated from measurements of the intensity of

the scattered beam,  $I$ , as a function of the scattering angle,  $2\theta$ . In actual practice the distance  $m$  of the detector above the primary beam is measured. This is related to the scattering angle by  $2\theta = m/a$  where  $a$  is the distance from the sample to the detector (20.5 cm). The complete mathematical treatment of the theory of small-angle x-ray scattering may be found in the works of Guinier and Fournet (6), Kratky (7), Luzzati (8), and Hendricks and Schmidt (9).

A North Carolina sandy soil, containing about 2 percent organic matter and very little clay, was extracted for 16 hours with 0.1N sodium hydroxide with a ratio of 1 part soil (by weight) to 10 parts solvent (by volume). The supernatant was centrifuged for 2 hours (7000 rev/min in a 31.1-cm, 28° rotor). Humic acid was repre-

cipitated at pH 1 with 6N hydrochloric acid and centrifuged again.

The precipitate was either lyophilized to obtain humic acid or dissolved in 0.1N sodium hydroxide to obtain sodium humate. The sodium humate was filtered through No. 1 Whatman paper and then through a 0.45- $\mu$  membrane filter. This filtrate was dialyzed (cellulose casing, 1.7-cm diameter, 25-Å pore) overnight against distilled water; the pH of the dialyzed sodium humate was 7.4. This was lyophilized. Solutions (percent in grams per 100 ml) were prepared by dissolving the humic acid in 0.1N sodium hydroxide and the sodium humate in water. All of the measurements were made with a Kratky small-angle scattering camera (7) mounted on a Sieman's x-ray generator equipped with a high-intensity copper x-ray tube. The scattered radiation intensity as a function of scattering angle was measured with a scintillation detector. The  $\text{CuK}\alpha$  radiation (1.54 Å) was isolated from the scattered beam by a pulse-height analyzer attached to the output of the scintillation detector (7). The x-ray beam was collimated with an entrance slit of 150  $\mu$  for most of the data. The entrance slit was reduced to 75  $\mu$  for some of the measurements at very small angles. Data were converted to absolute intensities by comparison with a standard polyethylene sample provided by O. Kratky. Either stainless steel sample-holders 1 mm thick with thin mica windows or glass capillaries 1 mm thick were used.

The Guinier curve,  $\log \bar{I}$  plotted against  $m^2$  (Fig. 1), consists of two different straight-line segments separated by a concave-up section. There

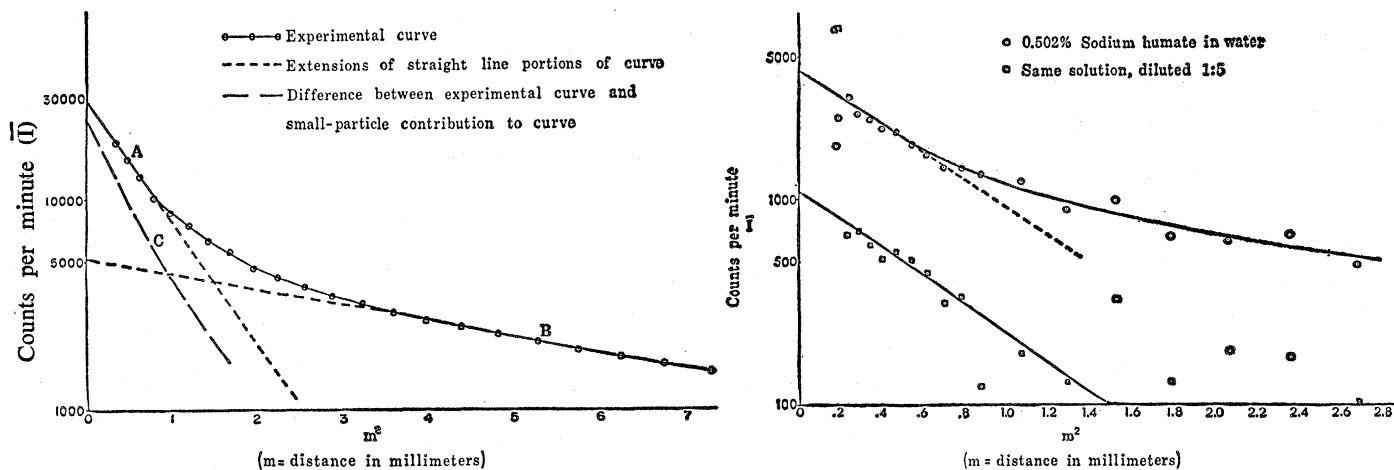


Fig. 1 (left). The log of scattered intensity,  $\bar{I}$ , measured in counts per minute, is plotted against distance from the primary beam to the detector, measured in millimeters and then squared,  $m^2$ . Slopes of the straight line portions of this Guinier plot are related to the radii of gyration of the scattering particles. Fig. 2 (right). A Guinier plot as in Fig. 1. This figure illustrates that identical slopes, that is, particle sizes, are obtained for straight line portions of the Guinier plot upon a 1 : 5 dilution.

are two possible interpretations of the Guinier curve (6, 7) because each straight-line portion of the curve corresponds to scattering taking place at the interface between zones of different electron density. There may be particles of different sizes or particles of uniform size consisting of distinct zones of different electron density. In order to determine which interpretation is correct we have made some preliminary column chromatographic studies with molecular sieves (Sephadex G-50, superfine).

This work indicates that this sodium humate solution contains three distinct fractions and that different particle sizes may exist. However, because sodium humate particles are highly charged, the molecular sieve columns may not be separating according to net charge or some as yet undetermined factor.

If the Guinier curve that was obtained for sodium humate is the sum of the scattering curves of several different size particles in solution, then the overlapping of these curves may obscure straight-line segments, other than the two shown in Fig. 1, and thus there is no contradiction between the three fractions that are observed by column chromatography and the two different size particles that are observed by small-angle x-ray scattering.

From the slope of the straight-line segments, the radius of gyration  $R_0$ , can be calculated. It will be noted that there is good agreement between the radii of gyration determined for the 0.5 percent sodium humate solutions and those of 0.3 and 0.6 percent humic acid solutions in sodium hydroxide. This suggests that sodium humate at different pH values exists in the same state. Measurements of sodium humate solutions made at very small angles with a 75- $\mu$  entrance slit yield an average maximum radius of gyration

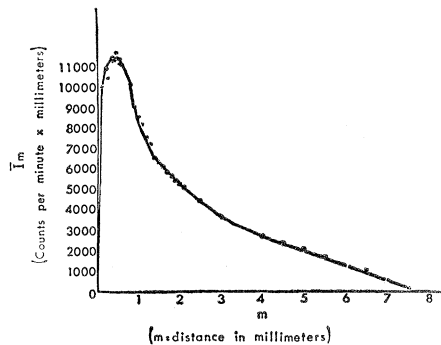


Fig. 3. The invariant,  $\bar{Q}$ , which is the area under the  $\bar{I}m$  versus  $m$  curve. The distance from the primary beam to the detector measured in millimeters is  $m^2$  and  $I$  is the scattering intensity measured in counts per minute. The invariant is corrected for collimation and used in calculation of molecular volume.

of about 110 Å. Both the larger and smaller radii of gyration measured for the 1.3-percent humic acid solution are larger than the corresponding radii for the less concentrated solutions. This difference may be due either to greater association of the molecules in the more concentrated solution or to concentration effects on the scattering. Extrapolation of the linear portions of the curve in Fig. 1 to  $m = 0$  yields two values of  $\bar{I}(m \rightarrow 0)$ . Figure 2 shows that the slopes, that is, the radii of gyration, are not appreciably changed by a 1:5 dilution. The  $\bar{I}(m \rightarrow 0)$  for the larger size particles is 30,000 count/min and that for smaller size is 5150 count/min. Kratky (7) has suggested that a graphical subtraction of the extrapolated intensity of the smaller particles ( $B$  portion of curve) from the total ( $A$  portion of curve) would yield the scattering of the larger particles (curve  $C$ ), Fig. 1. The curve resulting from this subtraction yields an  $\bar{I}(m \rightarrow 0)$  of 24,750 and a radius of gyration of 119 Å.

The radii of gyration obtained at very low angles and 100- $\mu$  detector slit are higher also than the 101 Å obtained from the  $A$  portion of the curve (Fig. 1).

The area under the  $\bar{I}m$  versus  $m$  curve in Fig. 3 is called the invariant and is used in calculating molecular volume (7, 8). The data plotted in Fig. 3 represent measurements taken at three different detector-slit widths (50  $\mu$ , 100  $\mu$ , and 150  $\mu$ ). It was necessary to use the slits of smaller widths for measurements of the scattering intensity at very small angles. All of the data have been normalized to a single slit width and primary beam width.

In order to calculate the volume of the scattering particles, the experimentally measured scattered intensity,  $\bar{I}(m \rightarrow 0)$ , obtained from a rectangular beam, was reduced to  $\bar{I}(m \rightarrow 0)$ , that obtained from a circular primary beam of infinitesimal diameter of an equivalent beam power (6-8). Unfortunately, we are not able at the present time to separate the large-particle and small-particle contributions to the invariant, and, therefore, the volumes calculated will be somewhat lower than they would be if we could evaluate the invariant for each of the sizes. The  $\bar{I}(m \rightarrow 0)$  values and the corresponding sizes, volumes, and molecular weights are summarized in Table 1. As a word of caution about the molecular weight values, it should be noted that the calculated volumes may be the volumes of micelles or hydrated molecules rather than those of the true molecular species. In order to calculate the molecular weight from the volume it was necessary to evaluate the density of the particles in solution. An isopycnic zonal centrifugation technique similar to that described by Anderson (10) was used for these density measurements. This technique separates particles according to their buoyant density independent of the particle sizes. The densities of the various particles are from 1.55 to 1.65 g/cm<sup>3</sup>. An average value of 1.6 g/cm<sup>3</sup> was used in the molecular weight calculations.

Although the exact shape of the humate ion cannot be obtained from these data, the ratio of the radius of gyration of the particle to the radius of gyration of a spherical particle of equal volume will be a measure of its deviation from spherical (Table 1). This ratio is called the shape factor,  $f$ . The values for  $f$  (1.3 to 2.5) indicate that the particles are ellipsoidal with the smaller particles being nearly spheroidal.

Table 1. The  $\bar{I}(m \rightarrow 0)$  values, sizes, volumes, and molecular weights of the samples.

Grams per 100 ml	$R_0$ (Å)	$\bar{I}(m \rightarrow 0)$	$V$ (Å <sup>3</sup> )	$M$	$f$
<i>Humic acid</i>					
1.25	137				
1.25	52				
0.63	114				
.63	48				
.25	101				
.25	36				
<i>Sodium humate</i>					
.50	101	$3.0 \times 10^4$	$1.2 \times 10^3$	$1.2 \times 10^6$	1.9
.50	38	$5.2 \times 10^3$	$2.1 \times 10^2$	$2.0 \times 10^5$	1.3
.50	119*	$2.5 \times 10^3$	$1.0 \times 10^3$	$9.7 \times 10^5$	2.5
.50	108†				
.10	110†				

\* Obtained by graphical subtraction of the intensity of the smaller particles from the total intensity.  
 † Measurements made only at very small angles with entrance slit reduced to 75  $\mu$ .

dal. This is similar to the findings of Flaig and Beutelspacher using electron microscopy (3).

In order to obtain more definitive knowledge about the size and shape of sodium humate molecules a homodisperse system must be obtained. Small-angle x-ray scattering offers a more specific means of characterizing humic acid preparations than others previously used.

R. L. WERSHAW  
P. J. BURCAR

U.S. Geological Survey,  
Denver, Colorado 80225

C. L. SUTULA  
B. J. WIGINTON

Denver Research Center,  
Marathon Oil Company,  
Littleton, Colorado 80120

#### References and Notes

1. C. Steelink, *J. Chem. Educ.* **40**, 379 (1963).
2. G. T. Felbeck, Jr., *Advances Agron.* **17**, 327 (1965).
3. W. Flaig and H. Beutelspacher, *Pflanzenenergie. Dueng. Bodenk.* **52**(97), 1 (1951).
4. R. W. Rex, *Nature* **188**, 1185 (1960); G. Tollin and O. Steelink, *Biochim. Biophys. Acta* **112**, 377 (1966).
5. B. R. Nagar, *Nature* **199**, 1213 (1963).
6. A. Guinier and G. Fournet, *Small Angle Scattering of X-Rays* (Wiley, New York, 1955).
7. O. Kratky, *Prog. Biophys. Chem.* **13**, 105 (1963).
8. V. Luzzati, *Acta Cryst.* **11**, 843 (1958).
9. R. W. Hendricks and P. W. Schmidt, *Acta Phys. Austriaca*, in press.
10. N. G. Anderson, *Nat. Cancer Inst. Monograph* **21**, 9 (1966).
11. We thank P. Dunton for suggesting the use of this technique, E. Evans, Dr. W. T. Lammer, and their associates for supplying the density measurements, D. Pinckney and S. Heller for technical assistance, and S. Booker for preparation of the manuscript. Publication authorized by the Director, U.S. Geological Survey.

20 April 1967; revised 7 August 1967 ■

## Tornadoes: Mechanism and Control

*Abstract. If electrical energy is invoked to account for the high velocity of tornadoes, hydrodynamics restricts the possible mechanisms of energy exchange. In particular, the vortex is driven by a line sink of electrically heated air that must extend at least 5 kilometers high. In those rare cases where heroic measures may be justified to protect a city in the path of a major tornado, some possible control measures are discussed in terms of the electrical heating mechanism.*

The possibility that the energy source of tornadoes is primarily electrical has been suggested independently by several authors, the most convincing analysis being given by Vonnegut (1). As he points out, this suggestion was made by Lucretius (2), but the more modern argument for an electrical energy mechanism is that purely hydrodynamic motion cannot adequately account for the very high wind speeds (close to Mach 1) derivable from the maximum available geostatic pressure potential of 0.1 atm. Abdullah (3) showed theoretically how a line sink in the atmosphere leads to an adiabatic vortex of constant angular momentum whose minimum critical radius is limited where the tangential air velocity reaches the speed of sound. Lewis and Perkins (4) showed how the observed pressure field around a tornado is entirely consistent with a frictionless vortex of specific, constant angular momentum ( $\Omega_0 = \omega R^2$ ) of approximately  $7.5 \times 10^7$  cm<sup>2</sup>/sec. This corresponds to the very small and reasonable ambient wind shear of  $\pm 4.8$  km/hour, 5 km either side of the tornado. The difficulty arises in explaining the line sink where the ratio of axial pressure to ambient pressure

is at least 1:2 when the maximum adiabatic pressure difference (including latent heat of condensation) is less than 0.1 atm ( $\Delta T \approx 30^\circ\text{C}$ ) from ground to the base of the tropopause. This pressure difference is the maximum pressure differential of the sink that can occur, provided the axial flow inside the vortex is frictionless from ground to the tropopause and provided that no mechanism for upgrading the specific energy is operating. This latter point concerning a mechanism for upgrading the specific energy content is analogous to the statement that no known hydrodynamic flow pattern allows one to create the equivalent of a jet engine operating stationary with respect to the atmosphere and with no mechanical moving parts. Mechanical (or electrical) leverage is always required to create a higher specific energy region from a lower specific energy source. The implication for a tornado is that a higher specific energy source than the adiabatic differential is necessary to give rise to the inferred line sink of 0.5 to 1 atm.

The presence of dramatic electrical effects associated with tornadoes has been reviewed (5). However, the magnetometer measurements discussed by

Brook (6) is the first strong evidence that the electrical energy involved is as large as the hydrodynamic dissipation. If we assume the pressure of the line sink is 0.5 atm and that the axial flow is one-half of sonic,  $C_0$ , within the critical radius defined by a tangential velocity of sound speed and the observed angular momentum of Lewis and Perkins, then

$$r_{crit} = \Omega_0 / C_0 = 25 \text{ m} \quad (1)$$

$$\text{Power} = P A U \approx 2 \times 10^{10} \text{ watts} \quad (2)$$

where the pressure,  $P$ , equals 0.5 atm; the area,  $A$ , equals  $\pi (r_{crit})^2$  which about equals  $2 \times 10^7$  cm<sup>2</sup>; and the axial velocity,  $U$ , equals  $1.6 \times 10^4$  cm/sec. As discussed by Brook, the magnetic field disturbance corresponds to several hundred amperes. At the mean potential difference of a thunderstorm cloud of  $10^8$  volts, this accounts for the observed tornado dissipation of  $2 \times 10^{10}$  watts. Rossow (7) suggested that this electrical energy is coupled to the vortex by a sheered horizontal current flow, and that this sheered stress furnishes the required angular momentum.

As it has already been pointed out, the ambient wind shear is more than adequate to supply the required angular momentum; second, the observed large currents discussed by Brook are vertical, as expected from the energy source of updraft convection, rather than horizontal; third, the very low viscosity assumed by Rossow of  $\eta_t$  (turbulent) of about  $0.1 \eta_l$  (laminar) for a Reynolds number of  $5 \times 10^9$  is unrealistically small. A better assumption for a quasistatically stable vortex is a viscosity such that the vortex decays in 50 to 100 revolutions. If this condition is used in Rossow's equations, the tangential vortex velocity,  $V$ , is limited such that

$$\rho_{air} V^2 / 2 \approx E^2 / 8\pi. \quad (3)$$

Indeed, any electrostatic configuration of acceleration is limited to condition 3 unless a mechanical constraint is imposed that results in a mechanical leverage. If electrostatic acceleration alone is used to create the axial line sink, then the pressure difference between the critical radius,  $r_{crit}$ , and outside at infinite radius is limited to

$$\Delta P = \int_{r_{crit}}^R E_r q dr \quad (4)$$

where  $q$  is the charge density,  $E_r$  is the radial field, and  $R$  is an outer maximum radius less than the length of the